

1 Determination of respiration and photosynthesis fractionation factors  
2 for atmospheric dioxygen inferred from a vegetation-soil-atmosphere  
3 analog of the terrestrial biosphere in closed chambers

4  
5 Clémence Paul<sup>1</sup>, Clément Piel<sup>2</sup>, Joana Sauze<sup>2</sup>, Nicolas Pasquier<sup>1</sup>, Frédéric Prié<sup>1</sup>, Sébastien Devidal<sup>2</sup>,  
6 Roxanne Jacob<sup>1</sup>, Arnaud Dapoigny<sup>1</sup>, Olivier Jossoud<sup>1</sup>, Alexandru Milcu<sup>2,3</sup>, Amaëlle Landais<sup>1</sup>

7  
8 <sup>1</sup>Laboratoire des Sciences du Climat et de l'Environnement, LSCE/IPSL, CEA-CNRS-UVSQ, Université Paris-  
9 Saclay, 91191 Gif-sur-Yvette, France

10 <sup>2</sup>Ecotron Européen de Montpellier (UAR 3248), Univ Montpellier, Centre National de la Recherche Scientifique  
11 (CNRS), Campus Baillarguet, Montferrier-sur-Lez, France

12 <sup>3</sup>Centre d'Ecologie Fonctionnelle et Evolutive, Univ Montpellier, CNRS, Univ Paul Valéry, EPHE, IRD, Montpellier,  
13 France

14  
15 Correspondence: Clémence Paul (clemence.paul@lsce.ipsl.fr)

16  
17 Abstract

18 The isotopic composition of dioxygen in the atmosphere is a global tracer which depends on the  
19 biosphere flux of dioxygen toward and from the atmosphere (photosynthesis and respiration) as well  
20 as exchanges with the stratosphere. When measured in fossil air trapped in ice cores, the relative  
21 concentration of <sup>16</sup>O, <sup>17</sup>O and <sup>18</sup>O of O<sub>2</sub> can be used for several applications such as ice core dating and  
22 past global productivity reconstruction. However, there are still uncertainties about the accuracy of  
23 these tracers as they depend on the integrated isotopic discrimination of different biological processes  
24 of dioxygen production and uptake, for which we currently have very few independent estimates.  
25 Here we determined the respiration and photosynthesis fractionation factors for atmospheric  
26 dioxygen from experiments carried out in a replicated vegetation-soil-atmosphere analog of the  
27 terrestrial biosphere in closed chambers with growing *Festuca arundinacea*. The values for <sup>18</sup>O  
28 discrimination during soil respiration and dark respiration in leaves are equal to  $-12.3 \pm 1.7$  ‰ and  
29  $-19.1 \pm 2.4$  ‰, respectively. In these closed biological chambers, we also found a value attributed to  
30 terrestrial photosynthetic isotopic discrimination equal to  $+3.7 \pm 1.3$  ‰. This last estimate suggests  
31 that the contribution of terrestrial productivity in the Dole effect may have been underestimated in  
32 previous studies.

## 34 1. Introduction

35 The oxygen cycle represents one of the most important biogeochemical cycles on Earth as oxygen is  
36 the second most important gaseous component in the atmosphere. Oxygen is an essential component  
37 for life on Earth as it is consumed by all aerobic organisms through respiration and produced by  
38 autotrophic organisms through photosynthesis.

39 The analysis of the oxygen isotopic composition classically expressed as  $\delta^{18}\text{O}$  and  $\delta^{17}\text{O}$  of  $\text{O}_2$  in air  
40 bubbles trapped in ice cores is currently used to provide information on the variations of the low  
41 latitude water cycle and the productivity of the biosphere during the Quaternary (Bender et al., 1994;  
42 Luz et al., 1999; Malaizé et al., 1999; Severinghaus et al., 2009; Blunier et al., 2002; Landais et al., 2010).  
43  $\delta^{18}\text{O}$  of  $\text{O}_2$  is also a very useful proxy for ice core dating through the resemblance of its variations with  
44 the variations of precession or summer insolation in the northern hemisphere (Shackleton, 2000;  
45 Dreyfus et al., 2007). These tracers are however complex and their interpretation relies on the precise  
46 knowledge of the various fractionation factors in the oxygen cycle.

47 First, interpreting the relationship between  $\delta^{18}\text{O}$  of  $\text{O}_2$  (or  $\delta^{18}\text{O}_{\text{atm}}$ ) variations in ice core air and the low  
48 latitude water cycle (e.g. Severinghaus et al., 2009; Landais et al., 2010; Seltzer et al., 2017) is still  
49 debated because of the multiple processes involved. Dole (1936) reported the relative atomic weight  
50 of oxygen in the air and water of Lake Michigan and gave as a measure of the  $\delta^{18}\text{O}$  value between both  
51 of about 21 ‰. Barkan and Luz (2005) showed that  $\delta^{18}\text{O}_{\text{atm}}$  is enriched compared to the  $\delta^{18}\text{O}$  of water  
52 of the global ocean (taken here as the Vienna Standard Mean Ocean Water, VSMOW) with a value of  
53 23.88 ‰. With the more recent values of Pack et al. (2017) of 24.15 ‰ and Wostbrock and Sharp (2021)  
54 of 24.05 ‰, we can envisage an enrichment of  $\delta^{18}\text{O}_{\text{atm}}$  with respect to VSMOW of about  $\sim 24$  ‰. This  
55 Dole effect is the result of several isotopic discriminations caused by biotic processes that enrich the  
56  $\delta^{18}\text{O}_{\text{atm}}$  relative to the oceanic values of water  $\delta^{18}\text{O}$ . First measurements have shown that the  
57 photosynthesis itself is not associated with a strong isotopic discrimination and produces oxygen with  
58 an isotopic composition which is close to the isotopic composition of the consumed water (Vinogradov  
59 et al., 1959; Stevens et al., 1975; Guy et al., 1993; Helman et al., 2005; Luz & Barkan, 2005). This is in  
60 contrast to the early results of Dole and Jenks (1959) who proposed a photosynthetic isotopic  
61 discrimination for plants and algae of 5 ‰. Vinogradov et al. (1959) challenged the results of Dole and  
62 Jenks (1944) by explaining that the  $^{18}\text{O}$  enrichment of  $\text{O}_2$  during their photosynthesis experiments is  
63 the result of contamination by atmospheric  $\text{O}_2$  and respiration. Guy et al. (1993) studied the  
64 photosynthetic isotopic discrimination on spinach thylakoids, cyanobacteria (*Anacystis nidulans*) and  
65 diatoms (*Phaeodactylum tricornutum*) and found on average only a slight isotopic discrimination of

66 0.3‰ which they considered negligible. Luz and Barkan (2005) also corroborates this idea by studying  
67 photosynthetic isotopic discrimination on *Philodendron* and did not obtain a  $^{18}\text{O}$  enrichment of the  $\text{O}_2$   
68 produced. This absence of isotopic discrimination can be theoretically explained by the process of  $\text{O}_2$   
69 generation within photosynthesis (photosystem II) involving water oxidation by the oxygen evolving  
70 complex (Tcherkez and Farquhar, 2007). For the oceanic biosphere, the isotopic composition of  $\text{O}_2$   
71 produced by photosynthesis is very close to the isotopic composition of the ocean. However, in  
72 terrestrial biosphere the  $\delta^{18}\text{O}$  of water split during photosynthesis (leaf water) is highly variable both  
73 spatially and temporally because of the decrease of  $\delta^{18}\text{O}$  of meteoric water toward higher latitudes  
74 (Dansgaard, 1974) and the enrichment in heavy isotopes in leaf water during evaporation (Dongmann  
75 et al., 1974). The mean  $\delta^{18}\text{O}$  enrichment of leaf water isotopic composition has been estimated  
76 between + 4.5 and + 6 ‰ with respect to the isotopic composition of mean global ocean water (Bender  
77 et al., 1994; Hoffmann et al., 2004). On top of this enrichment, the terrestrial and oceanic Dole effects  
78 are mostly explained by the respiratory isotopic discrimination of the order of magnitude of + 18 ‰  
79 (Bender et al., 1994).

80 Because of the isotopic enrichment in leaf water, the terrestrial Dole effect has been initially estimated  
81 to be 5 ‰ higher than the oceanic Dole effect and  $\delta^{18}\text{O}_{\text{atm}}$  used to estimate changes in the balance  
82 between land and marine productivity (Wang et al., 2008; Bender et al., 1994; Hoffmann et al., 2004).  
83 However, the evidence by Eisenstadt et al. (2010) of isotopic discrimination up to + 6‰ for marine  
84 phytoplankton photosynthesis rather suggests that the marine and terrestrial Dole effects are of the  
85 same order of magnitude. More specifically, Eisenstadt et al. (2010) determined several  
86 photosynthetic isotopic discrimination values depending on the phytoplankton studied  
87 (*Phaeodactylum tricornutum* = 4.5 ‰, *Nannochloropsis sp.* = 3 ‰, *Emiliania huxleyi* = 5.5 ‰ and  
88 *Chlamydomonas reinhardtii* = 7 ‰). If marine and terrestrial Dole effects are similar, then the past  
89 variations of  $\delta^{18}\text{O}_{\text{atm}}$  cannot be attributed to different proportions of terrestrial or marine Dole effects.  
90 They would be better related to low latitude water cycle influencing the leaf water  $\delta^{18}\text{O}$  consumed by  
91 photosynthesis and then the  $\delta^{18}\text{O}$  of  $\text{O}_2$  produced by this process (with a larger flux in the low latitude  
92 vegetated regions). This is supported by orbital and millennial variations of  $\delta^{18}\text{O}_{\text{atm}}$  in phase with calcite  
93  $\delta^{18}\text{O}$  in Chinese speleothem, a proxy strongly related to the intensity of hydrological cycle in South-  
94 East Asia (Severinghaus et al., 2009; Landais et al., 2010; Extier et al., 2018). The aforementioned  
95 studies show that qualitative and quantitative interpretation of  $\delta^{18}\text{O}_{\text{atm}}$  relies strongly on the estimate  
96 of  $\text{O}_2$  fractionation factors in the biological cycle but data to constrain the fractionation factors  
97 associated with respiration and photosynthesis for the different ecosystems are sparse.

98 In addition to the use of  $\delta^{18}\text{O}_{\text{atm}}$ , the combination of  $\delta^{17}\text{O}$  and  $\delta^{18}\text{O}$  of  $\text{O}_2$  provides a way to quantify  
99 variations in past global productivity (Luz et al., 1999). This method relies on the fact that  $\text{O}_2$ -

100 fractionating processes in the stratosphere and within the biosphere lead to different relationships  
101 between  $\delta^{17}\text{O}$  and  $\delta^{18}\text{O}$  of  $\text{O}_2$ . Oxygen is fractionated in a mass-independent manner in the  
102 stratosphere producing approximately equal  $^{17}\text{O}$  and  $^{18}\text{O}$  enrichments (Luz et al., 1999). On the  
103 contrary, the biosphere fractionating processes are mass-dependent such that the  $^{17}\text{O}$  enrichment is  
104 about half the  $^{18}\text{O}$  enrichment relative to  $^{16}\text{O}$ . We thus define a  $\Delta^{17}\text{O}$  anomaly as:

105

$$106 \quad \Delta^{17}\text{O} = \ln(1 + \delta^{17}\text{O}) - 0.516 \times \ln(1 + \delta^{18}\text{O}) \quad (1)$$

107

108  $\Delta^{17}\text{O}$  of  $\text{O}_2$  is equal to 0 by definition in the present-day troposphere (the standard for isotopic  
109 composition of atmospheric oxygen is the present-day atmospheric value).  $\Delta^{17}\text{O}$  of  $\text{O}_2$  is negative in  
110 the stratosphere and increases in biosphere productivity leads to an increase of  $\Delta^{17}\text{O}$  of  $\text{O}_2$ . As for the  
111 interpretation of  $\delta^{18}\text{O}_{\text{atm}}$ , the quantitative link between  $\Delta^{17}\text{O}$  of  $\text{O}_2$  and biosphere productivity depends  
112 on the exact fractionation factors associated with biosphere processes (Brandon et al., 2020).

113 Several studies have been conducted to estimate the fractionation factors during biosphere processes  
114 of  $\text{O}_2$  production and consumption. These fractionation factors are then implemented in global  
115 modeling approaches involving the use of models of global vegetation and oceanic biosphere for  
116 interpretation of  $\Delta^{17}\text{O}$  of  $\text{O}_2$  and  $\delta^{18}\text{O}_{\text{atm}}$  in term of environmental parameters (Landais et al., 2007;  
117 Blunier et al., 2012; Reutenauer et al., 2015; Brandon et al., 2020). Most of the fractionation factors  
118 used in these modeling approaches were obtained from studies conducted at the cell level:  
119 cyanobacterium (Helman et al., 2005), *E. coli* (Stolper et al., 2018), microalgae (Eisenstadt et al., 2010).  
120 In these studies, the underlying assumption is that the fractionation factor associated with  $\text{O}_2$   
121 measured at the cell level can be applied at the ecosystem scale. Yet, results from studies conducted  
122 at a larger scale, e.g. at the soil scale by Angert et al. (2001) found a global terrestrial respiratory  
123  $^{18}\text{O}/^{16}\text{O}$  of  $\text{O}_2$  discrimination for soil microorganisms varying between - 12 ‰ and - 15 ‰. This is lower  
124 than the - 18 ‰ discrimination classically used for respiration, with diffusion in soil playing a role in  
125 addition to the biological respiration isotopic discrimination. Angert and Luz (2001) also showed using  
126 experiments on roots of *Philodendron* plants and wheat seedlings that the respiratory discrimination  
127 of a soil with roots is lower (about - 12‰) than the - 18‰ discrimination associated with dark  
128 respiration. This is due to the low  $\text{O}_2$  concentration in roots whose presence favors a slower diffusion.  
129 Later, Angert et al. (2003) found an even larger spread of  $\text{O}_2$  isotopic discrimination in soil and showed  
130 that temperate and boreal soils have higher isotopic discrimination, respectively - 17.8‰ and -  
131 22.5‰.

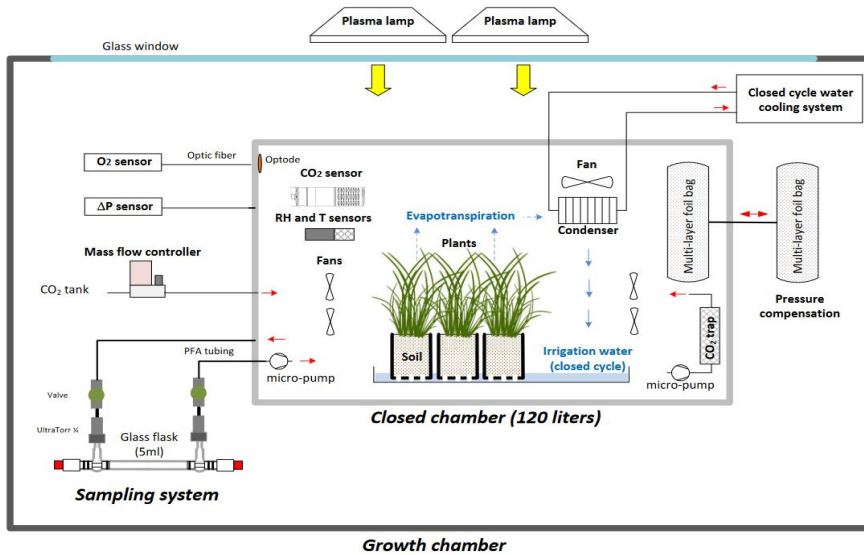
132 It has been suggested that the strong discrimination observed for boreal and temperate soils is due to  
133 the involvement of the alternative oxidase pathway (AOX, Bendall and Bonner, 1971) in addition to  
134 the usual COX respiratory pathway. In the COX respiration pathway, present in the majority in plants,  
135 the cytochrome oxidase enzyme catalyzes the oxygen reduction reaction. In the AOX pathway, the  
136 oxidation of ubiquinol molecules is directly coupled to the reduction of oxygen. Guy et al. (2005)  
137 showed that, for green tissues, the respiratory discrimination of the AOX pathway is much higher (-  
138 31‰) than the one of the COX pathway (- 21‰). Similarly, Ribas-Carbo et al. (1995) found a higher  
139 respiratory discrimination in phytoplankton that engage the AOX pathway (- 31 ‰) relative to bacteria  
140 that engage the COX pathway (- 24 ‰).

141 Other studies had attempted to investigate the different respiratory discriminations in the light (dark  
142 respiration, Mehler reaction and photorespiration). As during the light period, dark respiration can be  
143 inhibited (70 % inhibition found by Tcherkez et al. (2017) and Keenan et al. (2019)), so that the other  
144 O<sub>2</sub> consuming processes are important to consider. The Mehler reaction reduces oxygen to form a  
145 superoxide ion which is converted to hydrogen peroxide (H<sub>2</sub>O<sub>2</sub>) in photosystem I and then further  
146 converted to water (Mehler, 1951). Photorespiration is the result of the oxygenase activity of Rubisco  
147 (Sharkey, 1998). This enzyme can oxidize ribulose-1,5-bisphosphate with an oxygen molecule O<sub>2</sub>. This  
148 reaction causes a loss of CO<sub>2</sub> incorporation, thus decreasing the photosynthetic yield (Bauwe et al.,  
149 2010). Guy et al. (1993) first found a photorespiratory discrimination of - 21.7 ‰ and a <sup>18</sup>O/<sup>16</sup>O  
150 discrimination of - 15.3 ‰ for the Mehler reaction. Later, on a study performed on pea, Helman et al.  
151 (2005) found <sup>18</sup>O/<sup>16</sup>O discriminations of - 21.3 ‰ and - 10.8 ‰ respectively for photorespiration and  
152 Mehler reaction.

153 The above presented state of the art shows contrasting results for the determination of fractionation  
154 factors for the different photosynthesis and O<sub>2</sub> uptake processes, thus underlining the importance of  
155 performing new measurements to correctly interpret global variations of the isotopic composition of  
156 oxygen. Moreover, because there may be a difference between the fractionation factors at the cell  
157 level and at a broader level as shown for dark respiration in soil, we will favor here an approach at the  
158 scale of a terrarium including plant and soil.

159 In this study we developed a simplified vegetation-soil-atmosphere analog of the terrestrial biosphere  
160 in closed chamber of 120 dm<sup>3</sup> with the aim of estimating the fractionation factors of atmospheric  
161 dioxygen due to soil respiration, plant respiration and photosynthesis. With this setup we carried out  
162 several experimental runs with soil only and soil with plants in order to estimate the isotopic  
163 discrimination of the different compartments and check values obtained at the cell level. The  
164 implications for our interpretation of the Dole effect are also discussed.

165 2. Material and Methods  
 166 2.1. Growth chamber and closed system  
 167 2.1.1. Plant growth and experimental setup  
 168 a)



169  
 170 b)



171  
 172 Fig.1. A vegetation-soil-atmosphere analog of the terrestrial biosphere in a closed chamber. (a)  
 173 Schematic of the closed chamber setup used for the terrestrial biosphere model. The 120 dm<sup>3</sup> gas tight  
 174 closed chamber containing a terrestrial biosphere analogue is enclosed in a larger growth chamber  
 175 from the Ecotron Microcosms platform. Main environmental parameters inside the closed chamber

176 are actively controlled and monitored: temperature (T), light intensity, CO<sub>2</sub>, relative humidity (RH),  
177 pressure differential ( $\Delta P$ ). The water cycle in the closed chamber is shown in blue. (b) Photograph of  
178 the closed chamber used in the experiment with *Festuca arundinacea*.

179

180 Seeds of *Festuca arundinacea* (Schreb.), also commonly called tall fescue, were first sown in a  
181 commercial potting soil (Terreau universel, Botanic, France. Composition: black and blond peat, wood  
182 fibre, green compost and vermicompost manure, organic and organo-mineral fertilizers and  
183 micronutrient fertilizers). During 15 to 20 days, they were then placed in a growth chamber of the  
184 Microcosms experimental platform of the European Ecotron of Montpellier  
185 (<https://www.ecotron.cnrs.fr>) under diurnal light-dark cycles (Table S1), air temperature set at 20 °C  
186 ( $T_{air}$ ), air relative humidity (RH) at 80 % and CO<sub>2</sub> atmospheric concentration close to ambient air  
187 (concentration of CO<sub>2</sub> = 400 ppm).

188 Twelve pots (8 cm × 8 cm × 12 cm with 180 to 200 g of dry soil) containing approximately 25 to 30  
189 mature fescue plants were used for each experimental run. All plants were placed in a plastic tray filled  
190 with tap water, inside an airtight transparent chamber manufactured from welded polycarbonate (10  
191 mm wall thickness and 120 liters volume) similar to the chambers used by Milcu et al. (2013) (Fig. 1).  
192 The sealing of the closed chamber was checked before each experiment using helium.

193 To control temperature and light intensity inside the closed chamber, this smaller chamber was placed  
194 in a larger controlled environment growth chamber. Light was provided by two plasma lamps (GAVITA  
195 Pro 300 LEP02; GAVITA) with PAR = 200  $\mu\text{mol}\cdot\text{m}^{-2}\cdot\text{s}^{-1}$  and air temperature inside the closed chamber  
196 was regulated at  $19 \pm 1$  °C by adjusting the growth chamber temperature.

197 The closed chamber (Fig. 1) was used as a closed gas exchange system with controlled, and  
198 continuously monitored, environmental parameters. Air and soil temperature (CTN 35, Carel), air  
199 relative humidity (PFmini72, Michell instrument, USA) and CO<sub>2</sub> atmospheric concentration (GMP343,  
200 Vaisala, Finland) were measured and recorded using the growth chamber datalogger (sampling rate =  
201 1 min). O<sub>2</sub> concentration was continuously monitored using an optical sensor (Oxy1-SMA, Presens,  
202 Germany). Because precise O<sub>2</sub> concentration are determined in our samples by mass spectrometry  
203 (see next section), the measurements of the Oxy1-SMA were only used as a control during the  
204 experiment. The measured O<sub>2</sub> value for atmospheric air was adjusted to 20.9 % before each sequence  
205 of experiments and the same adjustment (offset) was then applied to the O<sub>2</sub> record during the  
206 following sequence.

207 Air relative humidity was regulated between 80 % and 90 % using a heat exchanger (acting as a  
208 condenser) connected to a closed cycle water cooling system. The condenser was positioned in a way  
209 to create a closed water cycle in the biological chamber (water vapor from evapotranspiration was  
210 condensed back into irrigation water). In order to keep the CO<sub>2</sub> mixing ratio close to 400 ppm during

211 the light periods, photosynthetic CO<sub>2</sub> uptake was compensated with injections of pure CO<sub>2</sub> using a  
212 mass flow controller (F200CV, Bronkhorst, The Netherlands). During the dark periods, a soda lime trap  
213 connected to a micro-pump (NMS 020B, KNF, Germany) was used to remove the excess CO<sub>2</sub> coming  
214 from respiration. CO<sub>2</sub> atmospheric concentration during the night was kept below 200 ppm.

215 To ensure atmospheric pressure stability in the closed chamber, a pressure compensation system,  
216 made of two connected 10 liters gas tight bags (Restek multi-layer polyvinyl fluoride foil gas sampling  
217 bag, USA), was installed. Each bag was half full of atmospheric air, the first one was installed in the  
218 closed chamber while the second one was outside this chamber. This way, each bag inflated or deflated  
219 in response to pressure variations caused either by O<sub>2</sub> or CO<sub>2</sub>, uptake or release. The pressure  
220 difference between the closed chamber and the atmosphere was regularly measured using a  
221 differential sensor (FD A602-S1K Almemo, Ahlborn, Germany).

222 Finally, the enclosed air was mixed using and considered homogeneous seven brushless fans.

223

## 224 2.1.2. Gas sampling

225

226 To measure the isotopic composition along the experiment, small samples of gas were collected in 5  
227 mL glass flasks, made of two Louwers H.V. glass valves (1-way bore 9mm Ref. LH10402008, Louwers  
228 Hanique, The Netherlands) welded together. Those flasks, previously evacuated, were mounted on  
229 PFA tubing (1/4<sup>th</sup>) using two 1/4<sup>th</sup> UltraTorr fitting (SS-4-UT-9, Swagelok, USA). Two manual valves (SS-  
230 4H, Swagelok, USA) were also installed on the PFA tubes to open or close the circuit. A micro-pump  
231 (NMS 20B, KNF, Germany) was finally turned on during air sampling to ensure closed chamber  
232 atmosphere circulation through the flask. The flow rate was equal to 1.6 L/min.

233

## 234 2.2. Isotopic measurements

### 235 2.2.1. Water extraction from leaf and isotopic analysis

236 After each experiment, the plant leaves were collected, placed in airtight flasks and immediately frozen  
237 at - 20°C for at least 24 hours to make sure there was minimal loss of water through vaporization when  
238 the vial was opened later. The extraction of water from leaves was done according to the procedure  
239 detailed in Alexandre et al. (2018). The vial was fixed onto a cryogenic extraction line and was first  
240 immersed in a liquid nitrogen Dewar to prevent any sublimation of the water. The water extraction  
241 line was emptied of most of its air ( $< 10^{-5}$  Pa). Once this pressure was reached, the pump was turned  
242 off and a valve was closed in order to keep a constant static void within the system. The “reception”  
243 vial was then immersed in a liquid nitrogen Dewar which will act as a water trap whilst the sample vial  
244 for the water was then transferred to a water bath maintained at 75°C. The system was kept in these



245 conditions for no less than six hours, so that all the water present in the leaf and stems was extracted.  
246 Afterwards, in order to remove all of the organic compounds of the extracted water, an active charcoal  
247 was placed in the extracted water and left under agitation for the night.

248 For analysis of  $\delta^{17}\text{O}$  and  $\delta^{18}\text{O}$  of water, leaf water was converted to  $\text{O}_2$  using a fluorination line for  
249 reaction of  $\text{H}_2\text{O}$  with  $\text{CoF}_3$  heated to  $370^\circ\text{C}$  at LSCE. The isotopic composition of the dioxygen was  
250 measured on an IRMS equipped with dual inlet (Thermo Scientific MAT253 mass spectrometer). The  
251 standard that was chosen was an  $\text{O}_2$  standard calibrated against VSMOW. The precision was  $0.015\text{‰}$   
252 for  $\delta^{17}\text{O}$ ,  $0.010\text{‰}$  for  $\delta^{18}\text{O}$  and  $6\text{ ppm}$  for  $\Delta^{17}\text{O}$  (Eq. (1)), for more details, refer to Landais et al. (2006).

253 The values of  $\delta^{18}\text{O}$  and  $\delta^{17}\text{O}$  of leaf water measured with respect to VSMOW are then expressed with  
254 respect to the isotopic composition of dioxygen in atmospheric air (classical standard for  $\delta^{18}\text{O}$  and  $\delta^{17}\text{O}$   
255 of  $\text{O}_2$  measurements). No consensus has been reached for the values of  $\delta^{18}\text{O}$  and  $\delta^{17}\text{O}$  of  $\text{O}_2$  in  
256 atmospheric air with respect to  $\delta^{17}\text{O}$  and  $\delta^{18}\text{O}$  of  $\text{H}_2\text{O}$  of VSMOW. These differences are most probably  
257 to be attributed to the different analytical techniques used for preparing and measuring the samples  
258 (Yeung et al., 2018; Wostbrock et al., 2021). In our case, because we use a similar set-up with the one  
259 developed by Barkan and Luz (2003) for the analyses of the triple isotopic composition of  $\text{O}_2$  in air (cf  
260 next section), we have chosen to base our calculation on their estimates. In this study, we have thus  
261 chosen the value of  $23.88\text{‰}$  for  $\delta^{18}\text{O}$  of  $\text{O}_2$  values with respect to VSMOW following (Barkan and Luz,  
262 2005). As for the  $\delta^{17}\text{O}$  of  $\text{O}_2$  value with respect to VSMOW value, we use two different possible  
263 estimates from these authors, either  $12.03\text{‰}$  (Luz and Barkan, 2011) or  $12.08\text{‰}$  (Barkan and Luz,  
264 2005). We acknowledge that because of the absence of consensus, slightly different values could be  
265 obtained for the fractionation factors determined in this study if a different choice is made for the  
266 reference values of  $\delta^{18}\text{O}$  and  $\delta^{17}\text{O}$  of  $\text{O}_2$  in atmospheric air with respect to  $\delta^{17}\text{O}$  and  $\delta^{18}\text{O}$  of  $\text{H}_2\text{O}$  of  
267 VSMOW.

#### 268 2.2.2. $\text{O}_2$ purification and isotopic analysis

269 The air samples collected in the closed chambers were transported to LSCE for analyses of the isotopic  
270 composition of  $\text{O}_2$ . The flasks were connected on a semi-automatic separation line inspired from  
271 Barkan and Luz (2003) which was made up of 8 ports in which 2 standards (outside air) and 6 samples  
272 were analyzed daily (Brandon et al., 2020). After pumping the whole line, the air was circulated through  
273 a water trap (ethanol at  $-100^\circ\text{C}$ ) and then through a carbon dioxide trap immersed in liquid nitrogen  
274 at  $-196^\circ\text{C}$ . After collection of the gas samples on a molecular sieve trap cooled at  $-196^\circ\text{C}$ , a helium  
275 flow carried it through a chromatographic column which was immersed in a water reservoir at  $0^\circ\text{C}$  to  
276 separate the dioxygen and the argon from the dinitrogen. After separation of the dioxygen and argon  
277 from helium, the gas was collected in a stainless-steel manifold immersed in liquid helium at  $-269^\circ\text{C}$ .

278 After collection, the samples were analyzed by the IRMS previously mentioned for leaf water analyses.  
 279 The following ratios were measured:  $^{18}\text{O}/^{16}\text{O}$ ,  $^{17}\text{O}/^{16}\text{O}$  and  $\text{O}_2/\text{Ar}$  (as an indicator of the  $\text{O}_2$   
 280 concentration because Ar is an inert gas).  $\delta^{17}\text{O}$  and  $\delta^{18}\text{O}$  of  $\text{O}_2$  each sample were obtained through 3  
 281 series of 24 dual inlet measurements against a standard made of  $\text{O}_2$  and Ar. This sequence was  
 282 followed by 2 peak jumping analyses of the  $\text{O}_2/\text{Ar}$  ratio including separate measurements of the  $\text{O}_2$  and  
 283 Ar signals for both the standard and the sample. The uncertainty associated with each measurement  
 284 was obtained from the standard deviation of the three runs and from the repeated peak jumping

285 measurement for  $\delta\text{O}_2/\text{Ar}$  which was defined by  $\left[ \frac{\left(\frac{n(\text{O}_2)}{n(\text{Ar})}\right)_{\text{sample}}}{\left(\frac{n(\text{O}_2)}{n(\text{Ar})}\right)_{\text{standard}}} - 1 \right] * 1000$ , and  $n(\text{O}_2)$  is the  
 286 number of moles of  $\text{O}_2$  and  $n(\text{Ar})$  the number of moles of Ar. The uncertainty values for  $\Delta^{17}\text{O}$ ,  $\delta^{18}\text{O}$   
 287 and  $\delta\text{O}_2/\text{Ar}$  were respectively 10 ppm, 0.05 ‰ and 0.5 ‰.

288 Each day, we performed measurements of the dioxygen isotopic composition and  $\text{O}_2/\text{Ar}$  ratio on two  
 289 samples of outside air which is the standard for the isotopic composition of  $\text{O}_2$  (Hillaire-Marcel et al.,  
 290 2021). So that the calibrated  $\delta^{18}\text{O}$  value for our sample was calculated as in equation 2:

291

$$292 \quad \delta^{18}\text{O}_{\text{calibrated}} = \left[ \frac{\left(\frac{\delta^{18}\text{O}_{\text{measured}}/1000\right)+1}{\left(\frac{\delta^{18}\text{O}_{\text{outsideair}}/1000\right)+1} - 1 \right] \times 1000 \quad (2)$$

293

## 294 2.3. Experimental runs

### 295 2.3.1. General strategy

296 Our goal was to calculate the fractionation factor associated with  $\delta^{17}\text{O}$  and  $\delta^{18}\text{O}$  for soil respiration,  
 297 dark leaf respiration and photosynthesis using the microcosm described above. In order to quantify  
 298 the fractionation factors, we needed to work in closed and controlled conditions. Given the volume of  
 299 the closed chamber ( $120 \text{ dm}^3$ , hence about 1.12 moles of  $\text{O}_2$ ) and the order of magnitude of dark  
 300 respiration (order of magnitude of  $0.08 \mu\text{mol O}_2 \text{ s}^{-1}$  for soil respiration) and net photosynthetic fluxes  
 301 (order of magnitude of  $0.45 \mu\text{mol O}_2 \text{ s}^{-1}$ ) inside the chamber, we calculated that experiments should  
 302 last from 3 days to more than 2 weeks so that more than one tenth of the  $\text{O}_2$  in the chamber can be  
 303 recycled by the plant and soil. This recycling allows the creation of sufficiently large isotopic signals  
 304 (especially  $\Delta^{17}\text{O}$  of  $\text{O}_2$ ) to be detected and measured. We set up two different experiments in the closed  
 305 chamber, each experiment being repeated 3 or 4 times to characterize the experimental repeatability  
 306 of the system.

307 The first experiment (repeated 4 times, i.e. in 4 sequences) aimed at studying the fractionation factors  
308 during soil respiration. The second experiment (repeated 3 times, i.e. in 3 sequences, each sequence  
309 being divided into several periods with or without light) aimed at studying the fractionation factors  
310 during dark respiration and photosynthesis of plants.

311 Prior to the aforementioned experiments, measurements were carried out on a closed empty chamber  
312 to check the absence of leaks as well as the absence of isotopic fractionation (Table S2).

313

### 314 2.3.2. Soil respiration experiment

315 To conduct the soil respiration experiment, 2.6 kg of soil (*Terreau universel, Botanic*) were placed in 12  
316 different pots. The light was turned off during this experimental run (Table S1). We decided not to  
317 apply any diurnal cycles during dark respiration experimentations for two reasons. First, we wanted to  
318 prevent the development of algae, mosses or any photosynthetic organisms in the chamber. Secondly,  
319 it was easier to optimize temperature control as the light radiation could increase the temperature  
320 inside the closed chamber. During this dark period, CO<sub>2</sub> from soil respiration accumulates in the  
321 biological closed chamber. To have a stable concentration of CO<sub>2</sub> during the whole dark period, the  
322 CO<sub>2</sub> was trapped using soda lime. Four sequences were performed with respective durations of 53, 51,  
323 43 and 36 days.

324

### 325 2.3.3. Photosynthesis and dark respiration experiment

326 We used the same soil with plants (*Festuca arundinacea*) grown before the start of the three  
327 sequences of the photosynthesis and dark respiration experiment. In order to obtain a significant  
328 change of the  $\Delta^{17}\text{O}$  of O<sub>2</sub> signal in our closed 120 dm<sup>3</sup> chambers, the 3 experiments were run for 1 to  
329 2 months. CO<sub>2</sub> level was controlled to 400 ppm by a CO<sub>2</sub> trap and CO<sub>2</sub> injections. This was done to  
330 ensure that the CO<sub>2</sub> in the chamber did not reach levels too far from the atmospheric composition as  
331 this could have affected the physiology of the plant. This could have affected the physiology of the  
332 plant. The light cycle was controlled to alternate between day (photosynthesis and respiration) and  
333 night conditions (respiration) (Table S1).

334 The values of the leaf water measurements are presented in supplementary Table S3. Because the  
335 experiments had to be carried in a closed chamber, we could not sample leaves during the experiment  
336 and only got a value at the end of each sequence. Nevertheless, we could compare the isotopic  
337 composition of the irrigation and soil water at the start and at the end of the experiment.

338

#### 339 2.4. Quantification of fractionation factors

340 We detail below how we used the results from our experiments to quantify the associated  
341 fractionation factors. Notations used below are gathered in Table 1.

342 The isotopic fractionation factor of oxygen is expressed through the fractionation factor  $\alpha$ .

343

$$344 \quad {}^{18}\alpha = \frac{{}^{18}R_{product}}{{}^{18}R_{substrat}} \quad (3)$$

345

346 where  $\alpha$  is the fractionation factor and  ${}^{18}R$  is the ratio of the concentration  ${}^{18}R = \frac{n({}^{18}O)}{n({}^{16}O)}$  with  $n$  the  
347 number of moles of  $O_2$  containing  ${}^{18}O$  or  ${}^{16}O$ .  ${}^{18}R$  is linked to the  $\delta^{18}O$  value through:

348

$$349 \quad \delta^{18}O = \left( \frac{{}^{18}R_{sample}}{{}^{18}R_{standard}} - 1 \right) \times 1000 \quad (4)$$

350

351 The isotopic discrimination is related to the isotopic fractionation factor through:

$$352 \quad {}^{18}\epsilon = {}^{18}\alpha - 1 \quad (5)$$

353 The same equations (3), (4) and (5) can be proposed for  $\delta^{17}O$  and the relationship between the  
354 fractionation factors  ${}^{17}\alpha$  and  ${}^{18}\alpha$  is written as:

$$355 \quad \theta = \frac{\ln {}^{17}\alpha}{\ln {}^{18}\alpha} \quad (6)$$

356 In some studies, referred to later, the notation  $\gamma$  is also used with  $\gamma = \frac{{}^{17}\epsilon}{{}^{18}\epsilon}$ .

##### 357 2.4.1. Soil respiration

358 Respiration is associated with isotopic fractionation. The light isotopes,  ${}^{16}O$ , are more easily integrated  
359 by microorganisms than the heavy isotopes,  ${}^{18}O$ , which hence remain in the atmosphere. We express  
360 the fractionation factor for soil respiration as:

361

362  $^{18}\alpha_{soil\_respi} = \frac{^{18}R_{respired}}{^{18}R_{air}}$  (7)

363

364 In our experiment, the respiratory process took place in a closed reservoir so that we could calculate  
 365 the fractionation factors from the evolution of the concentration and isotopic composition of dioxygen  
 366 in the chamber. The number of molecules of dioxygen in the air of the closed chamber,  $n(O_2)$ ,  
 367 between time  $t$  and time  $t+dt$  can be written as:

368

369  $n(O_2)_{t+dt} = n(O_2)_t - dn(O_2)$  (8)

370

371

372 with  $dn(O_2)$  the number of dioxygen molecules respired during the time period  $dt$ . A similar equation  
 373 can be written for the number of dioxygen molecules containing  $^{18}O$  remaining in the air of the  
 374 chamber:

375

376  $^{18}R_{t+dt} \times n(O_2)_{t+dt} = ^{18}R_t \times n(O_2)_t - ^{18}R_t \times ^{18}\alpha_{soil\_respi} \times dn(O_2)$  (9)

377

378 The evolution of the isotopic ratio of oxygen,  $^{18}R$ , between time  $t$  and time  $t+dt$  can be written as:

379

380  $^{18}R_{t+dt} = ^{18}R_t + d^{18}R$  (10)

381

382 Combining equations Eq. (8), (9) and (10), neglecting the second order term  $d^{18}R_t \times dn(O_2)_t$  and  
 383 integrating from  $t_0$  (starting time of the experiment when the chamber is closed) to  $t$  leads to:

384

385  $^{18}\epsilon_{soil\_respi} = ^{18}\alpha_{soil\_respi} - 1 = \frac{\ln\left(\frac{\frac{\delta^{18}O_{t+1}}{1000}}{\frac{\delta^{18}O_{t0+1}}{1000}}\right)}{\ln\left(\frac{n(O_2)_t}{n(O_2)_{t0}}\right)}$  (11)

386

387 Because argon is an inert gas, we can link  $\frac{n(O_2)_t}{n(O_2)_{t0}}$  to  $\delta\left(\frac{O_2}{Ar}\right)$ , so that:

388

389  $\frac{n(O_2)_t}{n(O_2)_{t0}} = \frac{\frac{\delta\left(\frac{O_2}{Ar}\right)_t + 1}{1000}}{\frac{\delta\left(\frac{O_2}{Ar}\right)_{t0} + 1}{1000}}$  (12)

390

391

392 2.4.2. Dark respiration

393 In order to calculate the isotopic fractionation associated with soil and plant respiration during dark  
394 period, we followed the same calculation as for the soil respiration (section 2.4.1). In this case, we  
395 selected only night periods from each sequence of the photosynthesis and dark respiration  
396 experiment.

397

398 2.4.3. Photosynthesis

399 During photosynthesis, the oxygen atoms in the dioxygen produced by the plant comes from the  
400 oxygen atom of water consumed by photosynthesis in the leaves so that the fractionation factor during  
401 photosynthesis can be expressed as:

402

$$403 \quad {}^{18}\alpha_{\text{photosynthesis}} = \frac{{}^{18}R_{\text{produced } O_2}}{{}^{18}R_{lw}} \quad (13)$$

404

405 where *lw* stands for leaf water.

406 For our study of *Festuca arundinacea* we consider that the water in the mesophyll layer can be  
407 represented by bulk leaf water.

408

409 Photosynthesis occurs during the light periods. However, it should be noted that dark respiration,  
410 photorespiration and Mehler reaction occur at the same time. In a first approach, we did the  
411 assumption that respiration rates remain the same during the light and dark periods. This  
412 assumption is probably true for soil respiration since flux of heterotrophic dark respiration is not  
413 expected to change for different light conditions if the other environmental drivers (e.g. humidity,  
414 temperature, soil organic matter) are constant. However, autotrophic dark respiration is expected to  
415 decrease during light periods compared to dark periods. As a consequence, we present sensitivity  
416 tests to the dependence of a vanishing dark respiration of leaves during the dark period in Table S4.

417

418 Thus, at each stage, dioxygen is both produced by photosynthesis and consumed by the  
419 aforementioned  $O_2$  uptake processes (hereafter *total\_respi*) by the plant according to the mass  
420 conservation equation:

421

$$422 \quad n(O_2)_{t+dt} = n(O_2)_t - dn_{\text{total\_respi}} + dn_{\text{photosynthesis}} \quad (14)$$

423

424 where  $dn_{total\_respi}$  is the number of molecules of  $O_2$  consumed by dark respiration, photorespiration  
425 and Mehler reaction between time  $t$  and  $t+dt$ , and  $dn_{photosynthesis}$  is the number of molecules of  $O_2$   
426 produced by photosynthesis between  $t$  and  $t+dt$ .

427

428 The budget for  $^{18}O$  of  $O_2$  can be written as:

429

$$430 \quad {}^{18}R_{t+dt} \times \frac{n(O_2)_{t+dt}}{n(O_2)_{t0}} = {}^{18}R_t \times \frac{n(O_2)_t}{n(O_2)_{t0}} - {}^{18}R_t \times {}^{18}\alpha_{total\_respi} \times \frac{dn_{total\_respi}}{n(O_2)_{t0}} + {}^{18}R_{lw} \times$$
$$431 \quad {}^{18}\alpha_{photosynthesis} \times \frac{dn_{photosynthesis}}{n(O_2)_{t0}} \quad (15)$$

432

433 where  ${}^{18}\alpha_{total\_respi}$  is the fractionation factors associated with each  $O_2$  consuming process periods  
434 throughout the whole experiment.

435 We introduced the normalized fluxes of photosynthesis and total respiration as:

436

$$437 \quad F_{photosynthesis} = \frac{dn_{photosynthesis}}{n(O_2)_{t0} \times dt} \quad (16)$$

438

$$439 \quad F_{total\_respi} = \frac{dn_{total\_respi}}{n(O_2)_{t0} \times dt} \quad (17)$$

440

$$441 \quad a^{18}R = \frac{d^{18}R}{dt} \quad (18)$$

442

443 This led to the following expression of  ${}^{18}\alpha_{photosynthesis}$  :

444

$$445 \quad {}^{18}\alpha_{photosynthesis} = \frac{n(O_2)_t / n(O_2)_{t0} \times a^{18}R + {}^{18}R_t \times (F_{photosynthesis} - F_{total\_respi} + {}^{18}\alpha_{total\_respi} \times F_{total\_respi})}{{}^{18}R_{lw} \times F_{photosynthesis}} \quad (19)$$

446

447 This equation can be simplified at  $t=0$  for  ${}^{18}R_t = {}^{18}R_{t0} = 1$  and  $n(O_2)_t = n(O_2)_{t0}$ :

450  ${}^{18}\alpha_{photosynthesis}$  depends on the values of  ${}^{18}\alpha_{total\_respi}$  and of  $F_{total\_respi}$ , themselves dependent  
451 on the values of  ${}^{18}\alpha_{Mehler}$  (fractionation factor associated with Mehler reaction),  $F_{Mehler}$  (flux of  
452 oxygen related to Mehler reaction),  ${}^{18}\alpha_{dark\_respi}$ ,  $F_{dark\_respi}$ ,  ${}^{18}\alpha_{photorespi}$  (fractionation factor  
453 associated with photorespiration) and  $F_{photorespi}$  (photorespiration flux of oxygen). These last 4

454 parameters could not be determined in our global experiment. Our determination of  $^{18}\alpha_{photosynthesis}$   
 455 will thus rely on assumptions for the estimations of  $^{18}\alpha_{Mehler}$ ,  $F_{Mehler}$ ,  $^{18}\alpha_{photorespi}$  and  $F_{photorespi}$ .  
 456

457 To separate the  $^{18}\alpha_{dark\_respi}$  from the other fractionation factors, we defined:

458

$$459 \quad ^{18}\alpha_{total\_respi} = ^{18}\alpha_{photorespi} \times f_{photorespi} + ^{18}\alpha_{Mehler} \times f_{Mehler} + ^{18}\alpha_{dark\_respi} \times f_{dark\_respi}$$

460 (20)

461 with

462

$$463 \quad F_{total\_respi} = F_{dark\_respi} + F_{photorespi} + F_{Mehler}$$

464 (21)

465

466  $f$  indicates the fraction of the total oxygen uptake flux corresponding to each process (dark  
 467 respiration, photorespiration and Mehler reaction) so that:

468

$$469 \quad f_{dark\_respi} + f_{photorespi} + f_{Mehler} = 1$$

470 (22)

471  $F_{dark\_respi} = f_{dark\_respi} \times F_{total\_respi}$  (23)

472

$$473 \quad F_{photorespi} = f_{photorespi} \times F_{total\_respi}$$

474 (24)

475  $F_{Mehler} = f_{Mehler} \times F_{total\_respi}$  (25)

476

477 In the absence of further constraints, we used here as first approximation the global values from  
 478 Landais et al. (2007) for  $f_{dark\_respi}$  (0.6),  $f_{photorespi}$  (0.3) and  $f_{Mehler}$  (0.1). Values for  $\alpha_{photorespi}$  and  
 479  $\alpha_{Mehler}$  were based on the most recent estimates of Helman et al. (2005).

480

481 Table 1. List of variables used to quantify fractionations and their definitions. \* means either oxygen  
 482 17 or oxygen 18.

Symbol	Definition	Origin of the value
* $\alpha$	Fractionation factor	



$^*\alpha_{dark\_respi}$	Fractionation factor of soil and plant respiration during night periods	Determined by our study
$^*\alpha_{dark\_leaf\_respi}$	Fractionation factor of leaf respiration during night periods	Determined by our study
$^*\alpha_{Mehler}$	Fractionation factor associated with Mehler respiration	Value from Helman et al. (2005)
$^*\alpha_{photorespi}$	Fractionation factor associated with photorespiration	Value from Helman et al. (2005)
$^*\alpha_{photosynthesis}$	Fractionation factor associated with photosynthesis	Determined by our study
$^*\alpha_{soil\_respi}$	Fractionation factor associated with soil respiration	Determined by our study
$^*\alpha_{total\_respi}$	Fractionation factor associated with total respiration during light period	Determined by our study
$^*\epsilon$	Isotopic discrimination	
$^*\epsilon_{dark\_respi}$	Isotopic discrimination of soil and plant respiration during night periods	Determined by our study
$^*\epsilon_{dark\_leaf\_respi}$	Isotopic discrimination of leaf respiration during night periods	Determined by our study
$^*\epsilon_{photosynthesis}$	Isotopic discrimination associated with photosynthesis	Determined by our study
$^*\epsilon_{soil\_respi}$	Isotopic discrimination of soil respiration associated with soil respiration experiment	Determined by our study
$\theta$	Ratio of $\ln(^{17}\alpha)$ to $\ln(^{18}\alpha)$	
$\theta_{dark\_respi}$	Ratio of $\ln(^{17}\alpha_{dark\_respi})$ to $\ln(^{18}\alpha_{dark\_respi})$	Determined by our study
$\theta_{dark\_leaf\_respi}$	Ratio of $\ln(^{17}\alpha_{dark\_leaf\_respi})$ to $\ln(^{18}\alpha_{dark\_leaf\_respi})$	Determined by our study
$\theta_{photosynthesis}$	Ratio of $\ln(^{17}\alpha_{photosynthesis})$ to $\ln(^{18}\alpha_{photosynthesis})$	Determined by our study
$\theta_{soil\_respi}$	Ratio of $\ln(^{17}\alpha_{soil\_respi})$ to $\ln(^{18}\alpha_{soil\_respi})$	Determined by our study

$aN$	Linear regression coefficient of the evolution of $n(O_2)$ as a function of time	Determined by our study
$a^*R$	Linear regression coefficient of the evolution of $R^*O$ as a function of time	Determined by our study
$dn_{photosynthesis}$	Number of moles of $O_2$ produced by photosynthesis between t and t+dt	Determined by our study
$dn_{total\_respi}$	Number of moles of $O_2$ consumed by total respiration during light periods between time t and t+dt	Determined by our study
$F_{dark\_respi}$	Dark respiration flux (normalized vs number of moles of $O_2$ at the start of the experiment)	Determined by our study
$F_{Mehler}$	Mehler flux (normalized vs number of moles of $O_2$ at the start of the experiment)	Determined by our study and Landais et al. (2007)
$F_{photorespi}$	Photorespiration $O_2$ flux (normalized vs number of moles of $O_2$ at the start of the experiment)	Determined by our study and Landais et al. (2007)
$F_{photosynthesis}$	Photosynthesis $O_2$ flux (normalized vs number of moles of $O_2$ at the start of the experiment)	Determined by our study
$F_{total\_respi}$	Total respiration $O_2$ flux during light period (normalized vs number of moles of $O_2$ at the start of the experiment)	Determined by our study
$f_{dark\_respi}$	Fraction of the dioxygen flux corresponding to dark respiration process	Value from Landais et al. (2007)
$f_{Mehler}$	Fraction of the dioxygen flux corresponding to Mehler process	Value from Landais et al. (2007)
$f_{photorespi}$	Fraction of the dioxygen flux corresponding to photorespiration process	Value from Landais et al. (2007)
$n(O_2)$	Number of moles of $O_2$	Determined by our study
$^*R$	Ratio of heavy ( $^{18}O$ or $^{17}O$ ) isotope to light isotope ( $^{16}O$ ) of $O_2$ in air	Determined by our study
$^*R_{lw}$	$^*R$ of leaf water	Determined by our study

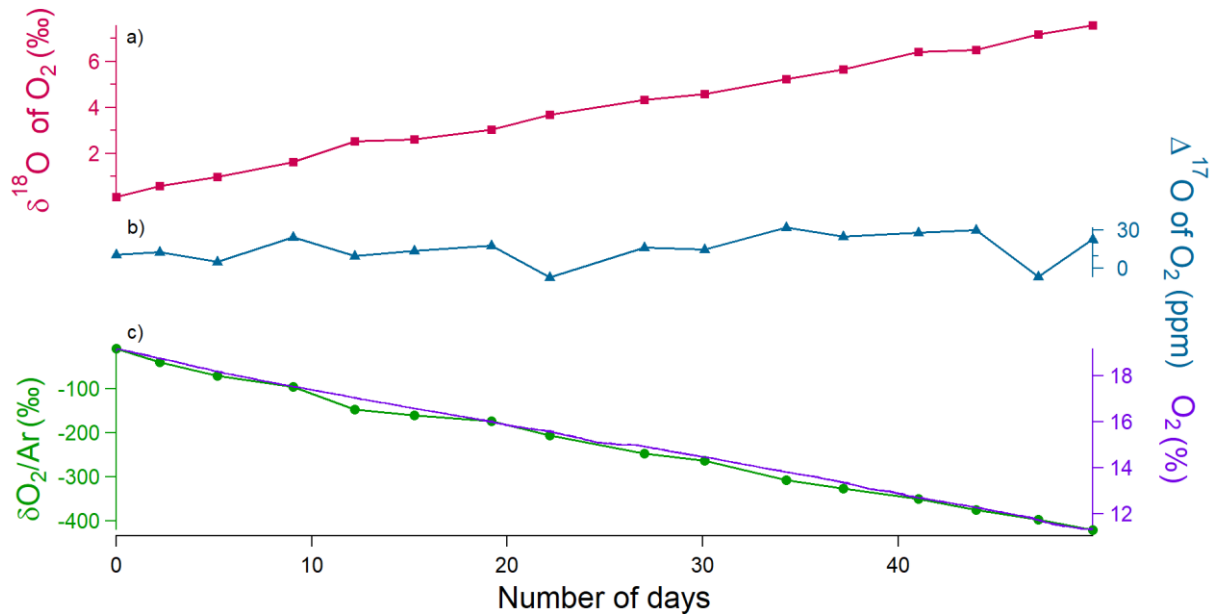
483

## 484 3.Results

### 485 3.1. Soil Respiration

#### 486 3.1.1. Experimental data

487



488

489

490 Fig.2. Evolution of the different concentrations and isotopic ratios in the sequence 2 of the soil  
491 respiration experiment (day 0 is the beginning of the sequence). (a)  $\delta^{18}\text{O}$  of  $\text{O}_2$  (red) variations. (b)  $\Delta^{17}\text{O}$   
492 of  $\text{O}_2$  (blue) variations. (c) Dioxygen concentration (purple) from the optical sensor and  $\delta\text{O}_2/\text{Ar}$   
493 variations (green) measured by IRMS.

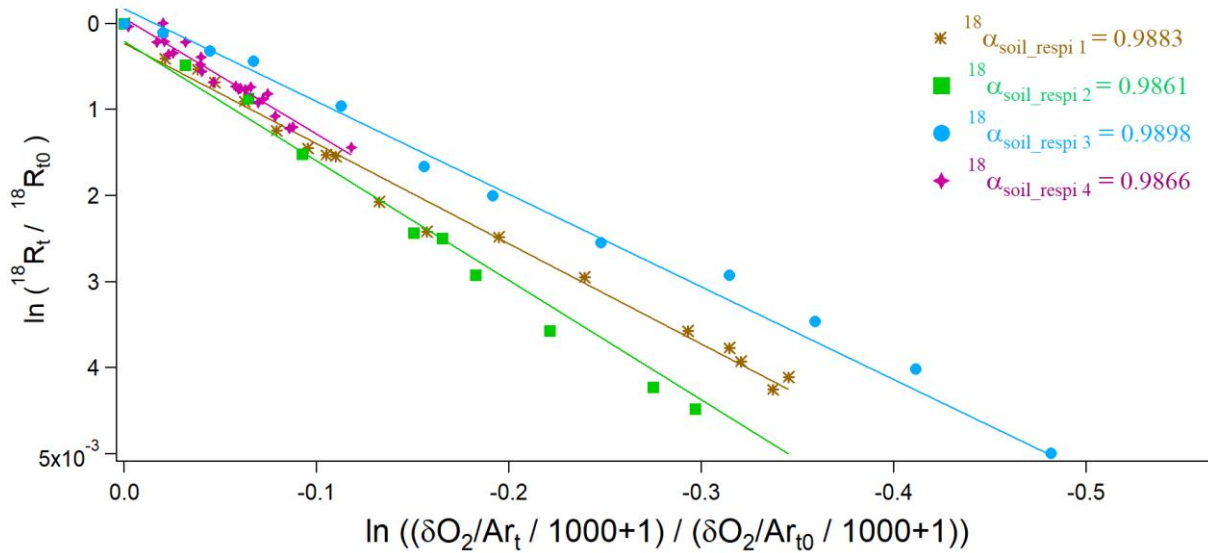
494 During the 4 sequences, the respiration activity led to a decreasing level of the  $\text{O}_2$  concentration  
495 measured by the optical sensor or through the  $\delta\text{O}_2/\text{Ar}$  evolution from IRMS measurements (Fig. S1).  
496 The comparison of the evolution of the  $\text{O}_2$  concentration during the different sequences showed that  
497 respiratory fluxes were different with a maximum factor of 4 between the different sequences (Fig.  
498 S1). In parallel to the decrease in  $\text{O}_2$  concentration, the  $\delta^{18}\text{O}$  increased as expected because respiration  
499 preferentially consumes the lightest isotopes: over the 51 days of the 2<sup>nd</sup> soil respiration sequence, we  
500 observed a linear decrease of oxygen concentration by more than 5 % while  $\delta^{18}\text{O}$  increased by 8 ‰  
501 (Fig. 2). A Mann-Kendall trend test showed that the  $\Delta^{17}\text{O}$  of  $\text{O}_2$  does not show any statistically  
502 significant trend over the 4 sequences (Fig. S2) (p-values were equal to 0.40, 0.08, 0.58, 0.47,  
503 respectively).

### 504 3.1.2. Fractionation factors

505 We used the 15 to 20 samples obtained during each sequence of soil respiration experiment to draw  
506 the relative evolution of  $\ln(^{18}\text{R}_t/^{18}\text{R}_{t_0})$  vs  $\ln((\delta(\frac{\text{O}_2}{\text{Ar}})_t/1000 + 1)/(\delta(\frac{\text{O}_2}{\text{Ar}})_{t_0}/1000 + 1))$   
507 following Eq. (11) (Fig. 3). The slope of the corresponding regression line provided the isotopic

508 discrimination  $^{18}\epsilon_{soil\_respi}$  and hence the fractionation factor  $^{18}\alpha_{soil\_respi}$  for each sequence (Table  
 509 S5). It could be observed that despite differences in respiratory fluxes for the different sequences (the  
 510 standard deviation is equal to 50 % of the average flux across sequences; see Table S5), the relationship  
 511 between  $\delta^{18}\text{O}$  of  $\text{O}_2$  and  $\text{O}_2$  concentration (or  $\delta\text{O}_2/\text{Ar}$ ), and hence the calculated fractionation factor  
 512 associated with respiration, is not much affected.

513



514

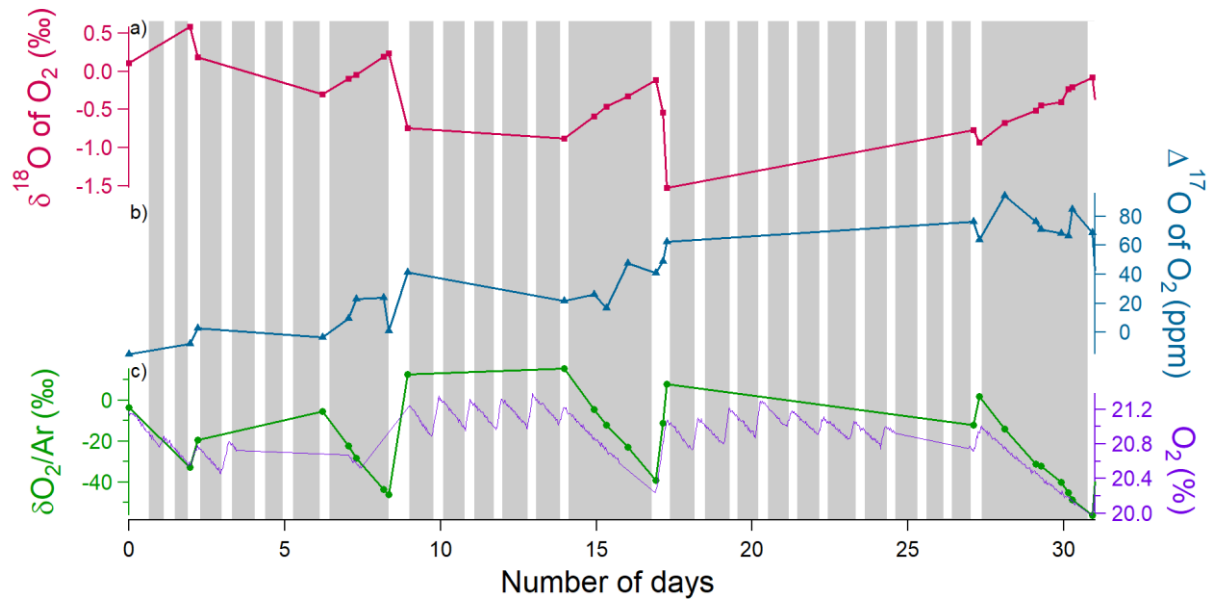
515 Fig.3 Determination of  $^{18}\text{O}/^{16}\text{O}$  fractionation factors in the 4 respiration sequences.  
 516  $^{18}\alpha_{soil\_respi\ 1}$  (brown),  $^{18}\alpha_{soil\_respi\ 2}$  (green),  $^{18}\alpha_{soil\_respi\ 3}$  (blue),  $^{18}\alpha_{soil\_respi\ 4}$  (purple) are  
 517 respectively respiratory fractionation factors associated with sequences 1 to 4.

518 Using the results of the 4 sequences, we determined the values for the mean isotopic discrimination  
 519  $^{18}\epsilon_{soil\_respi}$  ( $-12.3 \pm 1.7\text{‰}$ ), the mean isotopic discrimination  $^{17}\epsilon_{soil\_respi}$  ( $-6.4 \pm 0.9\text{‰}$ ) and the  
 520 average  $\theta_{soil\_respi}$  ( $0.5164 \pm 0.0005$ ).

521

## 522 3.2. Photosynthesis and dark respiration

### 523 3.2.1. Experimental data



524

525 Fig.4. Example of the evolution of the different concentrations and isotopic ratios in the sequence 1 of  
 526 photosynthesis and dark respiration experiment in the closed chamber over 31 days (day 0 is the  
 527 beginning of the sequence). Grey rectangles correspond to night periods and white rectangles to light  
 528 periods. (a)  $\delta^{18}\text{O}$  of  $\text{O}_2$  (red) variations. (b)  $\Delta^{17}\text{O}$  of  $\text{O}_2$  variations (blue). (c) Dioxygen concentration  
 529 (purple) from the optical sensor and  $\delta\text{O}_2/\text{Ar}$  variations (green) measured by IRMS.

530

531 During the night periods, when only respiration occurred, we observed a decrease in  $\text{O}_2$  concentration  
 532 by 1% within 3 days and a  $\delta^{18}\text{O}$  increase by 1‰ during the same period (Fig. 4). The evolution was  
 533 qualitatively similar with that of soil respiration experiments with higher fluxes. We observed the same  
 534 trends for the evolution of  $\delta\text{O}_2/\text{Ar}$  during the night periods as for the respiration experiment. During  
 535 light periods, there was a marked decrease in  $\delta^{18}\text{O}$  (2 ‰) and a marked increase in the flux of oxygen  
 536 released (1%) during 1 day. We observed the same trends for the evolution of  $\delta\text{O}_2/\text{Ar}$  during the night  
 537 periods as for the respiration experiment.

538

539 The Mann-Kendall test (95%) showed a significative increasing trend of the  $\Delta^{17}\text{O}$  of  $\text{O}_2$  over sequences  
 540 1 and 2 (Fig. S3) ( $\approx 100$  ppm in 31 days for sequence 1,  $\approx 100$  ppm in 40 days for sequence 2) while  
 541 no significant increase of  $\Delta^{17}\text{O}$  of  $\text{O}_2$  is observed over sequence 3 (Fig. S3).

542

### 543 3.2.2. Fractionation factors

#### 544 Dark respiration

545 The average of the isotopic discrimination for dark respiration  $^{18}\epsilon_{\text{dark\_respi}}$  and  $^{17}\epsilon_{\text{dark\_respi}}$  were  
 546 calculated over the 9 night periods and we obtained values of respectively  $-17.0 \pm 2.0$  ‰ and  $-8.5 \pm$

547 0.8 ‰. The average of  $\theta_{dark\_respi}$  during the experiment was equal to  $0.5124 \pm 0.0084$  (details in Table  
548 S6).

549 The dark respiration of this experiment includes respiration of both soil and leaves. Because soil  
550 respiration fractionation factor has been determined above, it is possible to estimate here the  
551 fractionation factor for the dark leaf respiration and we consider that respiration rate during dark and  
552 light periods do not vary:

553

$$554 F_{dark\_respi} = F_{soil\_respi} + F_{dark\_leaf\_respi} \quad (26)$$

$$555 {}^{18}\alpha_{dark\_respi} = f_{soil\_respi} \times {}^{18}\alpha_{soil\_respi} + f_{dark\_leaf\_respi} \times {}^{18}\alpha_{dark\_leaf\_respi} \quad (27)$$

556

557 with  $F_{dark\_leaf\_respi}$  the flux of leaf respiration during the night,  $f_{soil\_respi}$  the fraction of soil  
558 respiration during night periods ( $F_{soil\_respi} / F_{dark\_respi}$ ) and  $f_{dark\_leaf\_respi}$  the fraction of dark leaf  
559 respiration during night periods ( $F_{dark\_leaf\_respi} / F_{dark\_respi}$ ).

560

$$561 {}^{18}\alpha_{dark\_leaf\_respi} = \frac{{}^{18}\alpha_{dark\_respi} - f_{soil\_respi} \times {}^{18}\alpha_{soil\_respi}}{f_{dark\_leaf\_respi}} \quad (28)$$

562

563 The isotopic discriminations  ${}^{18}\epsilon_{dark\_leaf\_respi}$  and  ${}^{17}\epsilon_{dark\_leaf\_respi}$  were respectively equals to  $-19.1$   
564  $\pm 2.4$  ‰ and  $-9.7 \pm 0.9$  ‰. The average of  $\theta_{dark\_leaf\_respi}$  was equal to  $0.5089 \pm 0.0777$ . The standard  
565 deviations ( $1\sigma$ ) was calculated by a Monte Carlo method from the individual uncertainties of the  
566  ${}^{18}\alpha_{dark\_respi}$ ,  ${}^{18}\alpha_{soil\_respi}$ ,  $F_{soil\_respi}$  and  $F_{dark\_respi}$ .

567

## 568 Photosynthesis

569 In order to calculate an average value for the fractionation factor associated with photosynthesis from  
570 Eq. (19), we first calculated the averages of the flux of the  $O_2$  consuming processes and of the  
571 fractionation factors associated with each sequence:  $\langle F_{total\_respi} \rangle$  and  $\langle {}^{18}\alpha_{total\_respi} \rangle$ . We also  
572 calculated the net  $O_2$  flux during light periods,  $aN = F_{photosynthesis} - F_{total\_respi}$ , as the linear  
573 regression,  $aN$ , of  $\frac{n(O_2)_t}{n(O_2)_{t0}}$  with time.  $a^{18}R$  is also obtained as a linear regression of  ${}^{18}R$  with time over

574 each light period. Our data support our assumption that the regime was stationary over time and  
575  $n(O_2)_t / n(O_2)_{t0}$  evolved linearly over time, which is why we were able to do linear regressions.

576

$$577 \quad {}^{18}\alpha_{\text{photosynthesis}} = \frac{a^{18}R + aN + \langle {}^{18}\alpha_{\text{total\_respi}} \rangle \times \langle F_{\text{total\_respi}} \rangle}{{}^{18}R_{lw} \times F_{\text{photosynthesis}}} \quad (29)$$

578

579

580 The results of the 8 individuals  $\alpha_{\text{photosynthesis}}$  values are given in Table S10. The value of isotopic  
581 fractionation associated with the light period of period 1 of sequence 1 appeared clearly out of range.  
582 Following the Dixon's outlier detection test (Dixon, 1960), this value was considered an anomaly  
583 (likelihood > 99 %) and was removed from further analysis.

584

585 We finally estimated the values of  ${}^{18}\epsilon_{\text{photosynthesis}}$  and  ${}^{17}\epsilon_{\text{photosynthesis}}$  as  $+3.7 \pm 1.3 \text{ ‰}$  and  $+1.9$   
586  $\pm 0.6 \text{ ‰}$ , respectively. The average of  $\theta_{\text{photosynthesis}}$  was equal to  $0.5207 \pm 0.0537$ , a value which  
587 depends on the value taken for the  $\delta^{17}\text{O}$  value of atmospheric  $\text{O}_2$  vs VSMOW (Sharp and Wostbrock,  
588 2021), see Table 2.

589 We performed different sensitivity tests (supplementary texts 1 and 2). Sensitivity test 1 (Table S4)  
590 quantifies the influence of vanishing flux of dark leaf respiration during the day. This test shows that  
591 the assumption of similar flux of dark leaf respiration during the night and light periods did not  
592 influence much the values of photosynthesis fractionation factors. It results in an additional  
593 uncertainty of 0.0006 and 0.0005 for the values of  ${}^{18}\alpha_{\text{photosynthesis}}$  and  ${}^{17}\alpha_{\text{photosynthesis}}$ .

594 Sensitivity tests 2 (Tables S7, S8 and S9) were performed on values of the  $\text{O}_2$  flux and associated  
595 fractionation factors for photorespiration and Mehler reaction. They resulted in additional  
596 uncertainties of 0.0007 and 0.0005 for the values of  ${}^{18}\alpha_{\text{photosynthesis}}$  and  ${}^{17}\alpha_{\text{photosynthesis}}$  (Table  
597 S10).

598 Sensitivity tests 3 concerned the possible evolution of the isotopic composition of leaf water on the  
599 course of an experiment. The comparison of the  $\delta^{18}\text{O}$  of irrigation water and soil water at the end of  
600 the experiment shows a possible increase up to 2‰ (Table S3). We thus estimate that our values of  
601 leaf water  $\delta^{18}\text{O}$  measured at the end of the experiment may be overestimated by 1‰ compared to the  
602 mean value of leaf water  $\delta^{18}\text{O}$  during the course of the experiment. Taking this possible effect into  
603 account would lead to a fractionation factor for photosynthesis higher by 1‰ compared to the  
604 presented one of  $3.7 \pm 1.3 \text{ ‰}$ , hence a higher isotopic discrimination associated with photosynthesis.

605

606

607 Finally, we evaluated by a Monte Carlo calculation how the different uncertainties listed in the 3  
608 sensitivity tests described above influence the final uncertainty on the photosynthesis isotopic  
609 discrimination. We found a final standard deviations ( $1\sigma$ ) equal to 0.3 ‰ for  $^{18}\epsilon_{photosynthesis}$  and  
610 0.15 ‰ for  $^{17}\epsilon_{photosynthesis}$ .

611

## 612 4. Discussion

### 613 4.1. $\Delta^{17}\text{O}$ of $\text{O}_2$

614 The  $\Delta^{17}\text{O}$  of  $\text{O}_2$  is equal to 0 by definition for atmospheric air, and hence it should be equal to zero at  
615 the beginning of each experiment. The observed change during an experiment can only be driven by  
616 biological processes because the interaction with stratosphere is not possible in the closed chambers.

617 During the soil respiration experimental run, the  $\Delta^{17}\text{O}$  of  $\text{O}_2$  was constant. This directly reflects the  
618  $\theta_{soil\_respi}$  value of  $0.5164 \pm 0.0005$  (Table 2) because  $\Delta^{17}\text{O}$  of  $\text{O}_2$  is defined with a slope of 0.516  
619 between  $\ln(1 + \delta^{17}\text{O})$  and  $\ln(1 + \delta^{18}\text{O})$  (Eq. 1). This result is in good agreement and within the  
620 uncertainties given by Helman et al. (2005) with the  $\gamma$  value of 0.5174 (equivalent to a  $\theta$  of  $0.515 \pm$   
621  $0.0003$ ) obtained with respiration experiments on several micro-organisms.

622 During the experiment involving both oxygen uptake and photosynthesis, the  $\Delta^{17}\text{O}$  of  $\text{O}_2$  has a globally  
623 increasing trend with values reaching about 100 ppm after one month. Such behavior is expected and  
624 was already observed by Luz et al. (1999) with  $\Delta^{17}\text{O}$  of  $\text{O}_2$  values reaching 150 ppm after a 200-day  
625 experiment within a closed terrarium. This increase cannot be explained by respiration because  
626 respiration does not modify  $\Delta^{17}\text{O}$  of  $\text{O}_2$ . It can be explained by photosynthesis producing oxygen with  
627 a  $\Delta^{17}\text{O}$  of  $\text{O}_2$  different from the atmospheric one. Previous analyses have shown that the  $\Delta^{17}\text{O}$  of  $\text{H}_2\text{O}$   
628 of VSMOW (close to mean oceanic water) expressed vs isotopic composition of atmospheric  $\text{O}_2$  has a  
629 value between 134 to 223 ppm (using a definition of  $\Delta^{17}\text{O}$  of  $\text{H}_2\text{O} = \ln(1+\delta^{17}\text{O}) - 0.516 \times \ln(1+\delta^{18}\text{O})$ )  
630 (Sharp and Wostbrock, 2021). Within the water cycle, the slopes of  $\ln(1+\delta^{17}\text{O})$  vs  $\ln(1+\delta^{18}\text{O})$  for the  
631 meteoric line, evaporation and evapotranspiration lines are larger than 0.516 (Li and Meijer, 1998;  
632 Landais et al., 2006) so that  $\Delta^{17}\text{O}$  of water consumed by the plants during photosynthesis should be  
633 slightly lower than the  $\Delta^{17}\text{O}$  of VSMOW expressed vs isotopic composition of atmospheric  $\text{O}_2$  but still  
634 higher than the  $\Delta^{17}\text{O}$  of atmospheric  $\text{O}_2$ . Photosynthesis can thus explain the  $\Delta^{17}\text{O}$  of  $\text{O}_2$  increase in the  
635 closed chamber.

636

### 637 4.2. Fractionation factors associated with $\delta^{18}\text{O}$ of $\text{O}_2$ and implications for the Dole effect



638 Table 2. Summary of the mean values of the isotopic discriminations and gamma values for *Festuca*  
 639 *arundinacea* of all sequences of (1) the soil respiration experiment and of (2) the respiration and  
 640 photosynthesis experiment and the number of data on which they were calculated. \*\* is the value for  
 641  $\theta_{photosynthesis}$  that depends on the determination of the  $\delta^{17}O$  of atmospheric  $O_2$  vs  $\delta^{17}O$  of VSMOW.  
 642 We provide here the two different possible estimates using either 12.03 ‰ (Luz and Barkan, 2011) or  
 643 12.08 ‰ (Barkan and Luz, 2005): value determined with  $\delta^{17}O = 12.03$  ‰ / value determined with  $\delta^{17}O$   
 644 = 12.08 ‰.

645

Isotopic discriminations and gamma values of <i>Festuca arundinacea</i>	Average (‰)	Standard deviation (‰)	Number of data
$^{18}\epsilon_{soil\_respi}$	-12.3	1.7	4
$^{17}\epsilon_{soil\_respi}$	-6.4	0.9	4
$\theta_{soil\_respi}$	0.5164	0.0005	4
$^{18}\epsilon_{dark\_respi}$	-17.0	2.0	9
$^{17}\epsilon_{dark\_respi}$	-8.5	0.8	9
$\theta_{dark\_respi}$	0.5124	0.0084	9
$^{18}\epsilon_{dark\_leaf\_respi}$	-19.1	2.4	9
$^{17}\epsilon_{dark\_leaf\_respi}$	-9.7	0.9	9
$\theta_{dark\_leaf\_respi}$	0.5089	0.0777	9
$^{18}\epsilon_{photosynthesis}$	3.7	1.3	8
$^{17}\epsilon_{photosynthesis}$	1.9	0.6	8
$\theta_{photosynthesis}$	0.5207/0.5051**	0.0537/0.0504**	8

646

647 The isotopic discrimination  $^{18}\epsilon_{soil\_respi} = -12.3 \pm 1.7$  ‰ for the soil respiration experiments is  
 648 comparable to the average terrestrial soil respiration isotopic discrimination found by Angert et al.  
 649 (2001) of -12 ‰. Still, among the diversity of soils studied by Angert et al. (2001), the soils showing  
 650 the  $^{18}\epsilon$  values closest to our values are clay soil ( $^{18}\epsilon = -13$  ‰) and sandy soil ( $^{18}\epsilon = -11$  ‰). Soil  
 651 respiration isotopic discriminations are less strong than isotopic discrimination due to dark respiration  
 652 alone (-18 ‰, Bender et al., 1994). These lower values for soil respiration isotopic discrimination are  
 653 due to the roles of root diffusion in the soil (Angert and Luz, 2001). The soils studied by Angert and Luz  
 654 (2001) are however different from our soil which was enriched in organic matter. Further experiments  
 655 are then needed to understand the variability in  $^{18}\epsilon$  associated with soil respiration.

656 The isotopic discrimination for dark leaf respiration,  $^{18}\epsilon_{\text{dark\_leaf\_respi}} = -19.1 \pm 2.4 \text{ ‰}$  is associated  
657 with a large uncertainty and would benefit from additional experiments with a higher sampling and  
658 measurement rate. Still, even if it was obtained on different organisms and experimental set-ups, this  
659 value is in agreement with the values for isotopic discrimination for dark respiration determined by  
660 Helman et al. (2005) on bacteria from the Lake Kinneret ( $^{18}\epsilon = -17.1 \text{ ‰}$ ) and *Synechocystis* ( $^{18}\epsilon = -19.4$   
661  $\text{‰}$  and  $-19.5 \text{ ‰}$ ) and Guy et al. (1989) on *Phaeodactylum tricornutum* and on terrestrial plants ( $-17$  to  
662  $-19 \text{ ‰}$  for COX respiration).

663 The average  $^{18}\epsilon_{\text{photosynthesis}}$  is  $+3.7 \pm 1.3 \text{ ‰}$  for *Festuca arundinacea* species which goes against the  
664 classical assumption that terrestrial photosynthesis does not fractionate (Vinogradov et al., 1959; Guy  
665 et al., 1993; Helman et al., 2005; Luz & Barkan, 2005). Vinogradov explains that the low photosynthetic  
666 isotopic discrimination that can occur is due to contamination by atmospheric O<sub>2</sub> or by respiration.  
667 Guy et al. (1993) corroborate this idea by finding a photosynthetic isotopic discrimination of 0.3 ‰ in  
668 cyanobacteria (*Anacystis nidulans*) and diatoms (*Phaeodactylum tricornutum*) that they consider  
669 negligible. Luz and Barkan (2005) in their study on *Philodendron*, consider that there is no  
670 photosynthetic isotopic discrimination. Our value suggests that there is a terrestrial photosynthetic  
671 isotopic discrimination and the value found for *Festuca arundinacea* is slightly smaller than the  
672 photosynthetic isotopic discrimination in marine environment  $^{18}\epsilon_{\text{photosynthesis}} = +6 \text{ ‰}$  found by  
673 Eisenstadt et al. (2010). More specifically, Eisenstadt et al. (2010) determined several photosynthetic  
674 isotopic discrimination values depending on the phytoplankton studied (*Phaeodactylum tricornutum*  
675  $= 4.5 \text{ ‰}$ , *Nannochloropsis sp.*  $= 3 \text{ ‰}$ , *Emiliana huxleyi*  $= 5.5 \text{ ‰}$  and *Chlamydomonas reinhardtii*  $= 7$   
676  $\text{‰}$ ). One of the conclusions given by Eisenstadt et al. (2010) is that eukaryotic organisms enrich their  
677 produced oxygen more in <sup>18</sup>O than prokaryotic organisms. Our conclusion based on experiments  
678 performed with *Festuca arundinacea* species is in agreement with these conclusions.

679 Our experiments were performed at the scale of the plants which is different to previous studies  
680 performed at the scale of the chloroplast (e.g. Guy et al., 1993) where no evidence of oxygen  
681 fractionation has been found. We can thus not exclude that this fractionation attributed here to  
682 photosynthesis is due to oxygen consuming processes not taken into account in our approach. Our  
683 main goal however is to interpret the global  $\delta^{18}\text{O}$  of atmospheric O<sub>2</sub> using the fractionation observed  
684 at the scale of the plants. As a consequence, we believe that if there is a light-dependent oxygen  
685 fractionation process that we did not identify in our approach, it will also be present at the global scale.  
686 It should thus be taken into account in our future interpretation of the Dole effect. We thus keep our  
687 estimate of the photosynthesis <sup>18</sup>O discrimination described above but name it as an *effective*  
688 photosynthesis <sup>18</sup>O discrimination at the scale of the plants because the details of the processes at play  
689 is not fully elucidated.

690 Finally, we should however note that we tested only one species. Additional experiments with  
691 different plants are needed to check if the positive effective fractionation factor should be applied for  
692 global Dole effect calculation. Still, this positive *effective*  $^{18}\text{O}$  discriminations during photosynthesis  
693 suggests that the terrestrial Dole effect may be higher than currently assumed and challenge the  
694 assumption that terrestrial and oceanic Dole effects have the same values (Luz and Barkan, 2011).

695

## 696 4-Conclusion

697 Using a simplified analog of the terrestrial biosphere in a closed chamber we found that the  
698 fractionation factors of soil respiration and dark leaf respiration at the biological chamber level agree  
699 with the previous estimates derived from studies at micro-organism level. This is an important  
700 confirmatory step for the fractionation factors previously used to estimate the global Dole effect. More  
701 importantly, we document for the first time a significant *effective*  $^{18}\text{O}$  discrimination at the scale of the  
702 plant during terrestrial photosynthesis with the *Festuca arundinacea* species ( $+ 3.7 \text{ ‰} \pm 1.3 \text{ ‰}$ ). If  
703 confirmed by future studies, this can have a substantial impact on the calculation of the Dole effect,  
704 with important consequences for our estimates of the past global primary production.

705 Our study showed the usefulness of closed chamber systems to quantify the fractionation factors  
706 associated with biological processes in the oxygen cycle at the plant level. The main limitation of our  
707 present study was the low sampling rate during our experiments which hamper the precision of the  
708 determined fractionation factors. Future work should use this validated set-up to multiply such  
709 experiments to improve the precision of fractionation factors and to explore the variability of  
710 fractionation factors for different plants and hence different metabolisms. A good application would  
711 be to study the difference between C3 and C4 plants because C4 plants do not photorespire. C4 plants,  
712 adapted to dry environments, have their own strategy and make very little photorespiration through  
713 specialized cells. This allows them to produce their own energy in an optimal way without the waste  
714 produced by photorespiration.

715

## 716 Data availability

717 All individual fractionation factors for each experiment are given in the Supplement.

718

## 719 Author contributions

720 AL and CPi designed the project. CPi, JS and SD carried out experiments at ECOTRON of Montpellier  
721 and FP, CPa, RJ, AD and OJ at LSCE. CPa, NP and AL analyzed the data. CPa and AL prepared the  
722 manuscript with contributions from NP, CPi, JS and AM.

723

## 724 Competing interests

725 The authors declare that they have no conflict of interest.

726

## 727 Acknowledgements

728 The research leading to these results has received funding from the European Research Council under  
729 the European Union H2020 Programme (H2020/20192024)/ERC grant agreement no. 817493 (ERC  
730 ICORDA) and ANR HUM17. The authors acknowledge the scientific and technical support of PANOPLY  
731 (Plateforme ANalytique géOsciences Paris-sacLaY), Paris-Saclay University, France. This study  
732 benefited from the CNRS resources allocated to the French ECOTRONS Research Infrastructure, from  
733 the Occitanie Region and FEDER investments as well as from the state allocation 'Investissement  
734 d'Avenir' AnaEE- France ANR-11-INBS-0001. We would also like to thank Abdelaziz Faez and Olivier  
735 Ravel from ECOTRON of Montpellier for their help, Anne Alexandre from CEREGE at Aix-en-Provence  
736 and Emeritus Prof. Phil Ineson from University of York.

737

## 738 References

739 Alexandre, A., Landais, A., Vallet-Coulomb, C., Piel, C., Devidal, S., Pauchet, S., Sonzogni, C., Couapel,  
740 M., Pasturel, M., Cornuault, P., Xin, J., Mazur, J-C., Prié, F., Bentaleb, I., Webb, E., Chalié, F., and Roy,  
741 J.: The triple oxygen isotope composition of phytoliths as a proxy of continental atmospheric  
742 humidity: insights from climate chamber and climate transect calibrations, *Biogeosciences*, 15,  
743 3223-3241, <https://doi.org/10.5194/bg-15-3223-2018>, 2018.

744

745 Angert, A., Luz, B., and Yakir, D.: Fractionation of oxygen isotopes by respiration and diffusion in  
746 soils and its implications for the isotopic composition of atmospheric O<sub>2</sub>, *Global Biogeochem. Cy.*,  
747 15, 871-880, <https://doi.org/10.1029/2000GB001371>, 2001.

748

749 Angert, A., Barkan, E., Barnett, B., Brugnoli, E., Davidson, E. A., Fessenden, J., Maneepong, S.,

750 Panapitukkul, N., Randerson, J. T., Savage, K., Yakir, D., and Luz, B.: Contribution of soil respiration in  
751 tropical, temperate, and boreal forests to the  $^{18}\text{O}$  enrichment of atmospheric  $\text{O}_2$ , *Global*  
752 *Biogeochem. Cy.*, 17, 1089, <https://doi.org/10.1029/2003GB002056>, 2003.  
753

754 Barkan, E., and Luz, B.: High precision measurements of  $^{17}\text{O}/^{16}\text{O}$  and  $^{18}\text{O}/^{16}\text{O}$  of  $\text{O}_2$  and  $\text{O}_2/\text{Ar}$  ratio in  
755 air, *Rapid Commun. Mass Spectrom.*, 17, 2809-2814, <https://doi.org/10.1002/rcm.1267>, 2003.  
756

757 Barkan, E., and Luz, B.: High precision measurements of  $^{17}\text{O}/^{16}\text{O}$  and  $^{18}\text{O}/^{16}\text{O}$  ratios in  $\text{H}_2\text{O}$ , *Rapid*  
758 *Commun. Mass Spectrom.*, 19, 3737-3742, <https://doi.org/10.1002/rcm.2250>, 2005.

759 Bauwe, H., Hagemann, M., and Fernie, A.R.: Photorespiration: players, partners and origin, *Trends*  
760 *Plant Sci.*, 6, 330-336, <https://doi.org/10.1016/j.tplants.2010.03.006>, 2010.

761 Bender, M., Sowers, T., Dickson, M-L., Orchardo, J., Grootes, P., Mayewski, P. A., and Meese, D. A.:  
762 Climate correlations between Greenland and Antarctica during the past 100,000 years, *Nature*, 372,  
763 663-666, <https://doi.org/10.1038/372663a0>, 1994.  
764

765 Blunier, T., Barnett, B., Bender, M. L., and Hendricks, M. B.: Biological oxygen productivity during the  
766 last 60,000 years from triple oxygen isotope measurements, *Global Biogeochem. Cy.*, 16, 3-4,  
767 <https://doi.org/10.1029/2001GB001460>, 2002.  
768

769 Brandon, M., Landais, A., Duchamp-Alphonse, S., Favre, V., Schmitz, L., Abrial, H., Prié, F., Extier, T.,  
770 and Blunier, T.: Exceptionally high biosphere productivity at the beginning of Marine Isotopic Stage  
771 11, *Nat. Commun.*, 11, 1-10, <https://doi.org/10.1038/s41467-020-15739-2>, 2020.  
772

773 Dansgaard, W.: Stable isotopes in precipitation, *Tellus*, 16, 436-468, 1974.  
774

775 Davidson, E.A., Janssens, I.A., and Luo, Y.: On the variability of respiration in terrestrial ecosystems:  
776 moving beyond Q10, *Glob. Change Biol.*, 12, 154-164, [https://doi.org/10.1111/j.1365-](https://doi.org/10.1111/j.1365-2486.2005.01065.x)  
777 [2486.2005.01065.x](https://doi.org/10.1111/j.1365-2486.2005.01065.x), 2005.  
778

779 Dixon, W. J.: Simplified estimation from censored normal sample, *Ann. Math. Stat.*, 21, 488-506,  
780 <https://doi.org/10.1214/aoms/1177729747>, 1960.  
781

782 Dole, M.: *The Relative Atomic Weight of Oxygen in Water and in Air A Discussion of the Atmospheric*  
783 *Distribution of the Oxygen Isotopes and of the Chemical Standard of Atomic Weights*, J. Chem. Phys.  
784 4, 268, <https://doi.org/10.1063/1.1749834>, 1936.  
785  
786  
787 Dongman, G., Nürnberg, H. W., Förstel, H., and Wagener, K.: On the enrichment of H<sub>2</sub><sup>18</sup>O in the  
788 leaves of transpiring plants, *Radiat Environ Biophys*, 11, 41-52,  
789 <https://doi.org/10.1007/BF01323099>, 1974.  
790  
791 Dreyfus, G. B., Parrenin, F., Lemieux-Dudon, B., Durand, G., Masson-Delmotte, V., Jouzel, J.,  
792 Barnola<sup>3</sup>, J-M., Panno<sup>5</sup>, L., Spahni, R., Tisserand, A., Siegenthaler, U., and Leuenberger, M.:  
793 Anomalous flow below 2700 m in the EPICA Dome C ice core detected using δ<sup>18</sup>O of atmospheric  
794 oxygen measurements, *Clim. Past*, 3, 341-353, <https://doi.org/10.5194/cp-3-341-2007>, 2007.  
795  
796 Eisenstadt, D., Barkan, E., Luz, B., and Kaplan, A.: Enrichment of oxygen heavy isotopes during  
797 photosynthesis in phytoplankton, *Photosynth. Res.*, 103, 97-103,  
798 <https://doi.org/10.1007/s11120-009-9518-z>, 2010.  
799  
800 Extier, T., Landais, A., Bréant, C., Prié, F., Bazin, L., Dreyfus, G., Roche, D. M., and Leuenberger, M.:  
801 On  
802 the use of δ<sup>18</sup>O<sub>atm</sub> for ice core dating, *Quat. Sci. Rev.*, 185, 244-257,  
803 <https://doi.org/10.1016/j.quascirev.2018.02.008>, 2018.  
804  
805 Guy, R. D., Fogel, M.L., and Berry, J. A.: Photosynthetic fractionation of the stable isotopes of oxygen  
806 and carbon, *Plant Physiol.*, 101, 37-47, <https://doi.org/10.1104/pp.101.1.37>, 1993.  
807  
808 Helman, Y., Barkan, E., Eisenstadt, D., Luz, B., and Kaplan, A.: Fractionation of the three stables  
809 oxygen isotopes by oxygen-producing and oxygen-consuming reactions in photosynthetic  
810 organisms, *Plant Physiol.*, 138, 2292-2298, <https://doi.org/10.1104/pp.105.063768>, 2005.  
811  
812 Hillaire-Marcel, C., Kim, S-T., Landais, A., Ghosh, P., Assonov., S., Lécuyer, C., Blanchard, M., Meijer,  
813 H. A. J., and Steen-Larsen, H.: A stable isotope toolbox for water and inorganic carbon cycle studies,  
814 *Nat. Rev. Earth Environ*, 2, 699-719, <https://doi.org/10.1038/s43017-021-00209-0> , 2021.  
815  
816 Hoffmann, G., Cuntz, M., Weber, C., Ciais, P., Friedlingstein, P., Heimann, M., Jouzel, J., Kaduk, J.,

817 Maier Reimer, E., Seibt, U., and Six, K.: A model of the Earth's Dole effect, *Global Biogeochem. Cy.*,  
818 18, 1-15, <https://doi.org/10.1029/2003GB002059>, 2004.

819 Keenan, T.F., Migliavacca M., Papale, D., Baldocchi, D., Reichstein, M., Torn, M., and Wutzler, T.:  
820 Widespread inhibition of daytime ecosystem respiration, *Nat. Ecol. Evol.*, 3, 407-415,  
821 <https://doi.org/10.1038/s41559-019-0809-2>, 2019.

822

823 Landais, A., Barkan, E., Yakir, D., and Luz, B.: The triple isotopic composition of oxygen in leaf water,  
824 *Geochim. Cosmochim. Ac.*, 70, 4105-4115, <https://doi.org/10.1016/j.gca.2006.06.1545>, 2006.

825

826 Landais, A., Dreyfus, G., Capron, E., Masson-Delmotte, V., Sanchez-Goñi, M. F., Desprat, S.,  
827 Hoffmann, G., Jouzel, J., Leuenberger and M., Johnsen, S.: What drives the orbital and millennial  
828 variations of  $d^{18}O_{atm}$ ?, *Quat. Sci. Rev.*, 29, 235-246, <https://doi.org/10.1016/j.quascirev.2009.07.005>,  
829 2010.

830

831 Luz, B., and Barkan, E.: The isotopic composition of atmospheric oxygen, *Global Biogeochem. Cy.*,  
832 25, GB3001, <https://doi.org/10.1029/2010GB003883>, 2011.

833

834 Luz, B., Barkan, E., Bender, M. L., Thieme, M. H., and Boering, K. A.: Triple-isotope composition of  
835 atmospheric oxygen as a tracer of biosphere productivity, *Nature*, 400, 547-550,  
836 <https://doi.org/10.1038/22987>, 1999.

837

838 Malaizé, B., Paillard, D., Jouzel, J., and Raynaud, D.: The Dole effect over the Last two glacial-  
839 interglacial cycles, *J. Geophys. Res.*, 104, 14199-14208, <https://doi.org/10.1029/1999JD900116>,  
840 1999.

841 Mehler, A.: Studies on reactions of illuminated chloroplasts: I. Mechanism of the reduction of  
842 oxygen and other hill reagents, *Arch. Biochem. Biophys.*, 33, 65-77,  
843 [https://doi.org/10.1016/00039861\(51\)90082-3](https://doi.org/10.1016/00039861(51)90082-3), 1951.

844

845 Meijer, H. A. J., and Li, W. J.: The use of electrolysis for accurate  $\delta^{17}O$  and  $\delta^{18}O$  Isotope  
846 Measurements in Water, *Isot. Environ. Health Stud.*, 34, 349-369,  
847 <https://doi.org/10.1080/10256019808234072>, 1998.

848

849 Milcu, A., Allan, E., Roscher, C., Jenkins, T., Meyer, S. T., Flynn, D., Bessler, H., Buscot, F.,

850 Engels, C., Gubsch, M., König, S., Lipowsky, A., Loranger, J., Renker, C., Scherber, C., Schmid,  
851 B., Thébault, E., Wubet, T., Weisser, W. W., Scheu, S., and Eisenhauer, N.: Functionally and  
852 phylogenetically diverse plant communities key to soil biota, *Ecology*, 94, 1878-1885,  
853 <https://doi.org/10.1890/12-1936.1>, 2013.

854 Pack, A., Höweling, A., C.Hezel, D., T.Stefanak, M., Beck, A-K., T. M.Peters, S., Sengupta, S., Herwartz,  
855 D., and Folco, L.: Tracing the oxygen isotope composition of the upper Earth's atmosphere using  
856 cosmic spherules, *Nat. Commun*, 8, 1502, <https://doi.org/10.1038/ncomms15702>, 2017.  
857  
858

859 Reutenauer, C., A. Landais, A., T. Blunier, T., C. Bréant, C., M. Kageyama, M., M.-N. Woillez, M-N.,  
860 Risi, C., Mariotti, V., and P. Braconnot, Quantifying molecular oxygen isotope variations during a  
861 Heinrich stadial, *Clim. Past*, 11, 1527-1551, <https://doi.org/10.5194/cp-11-1527-2015>, 2015.  
862

863 Ribas-Carbo, M., Berry, J.A., Yakir, D., Giles, L., Robinson, S.A., Lennon, A.M., and Siedow, J.N.:  
864 Electron Partitioning between the Cytochrome and Alternative Pathways in Plant  
865 Mitochondria, *Plant Physiol.*, 109, 829-837, <https://doi.org/10.1104/pp.109.3.829>, 1995.  
866

867 Seltzer, A. M., Severinghaus, J. P., Andraski, B. J., and Stonestrom, D. A.: Steady state  
868 fractionation of heavy noble gas isotopes in a deep unsaturated zone, *Water Resour. Res.*, 53,  
869 2716-2732, <https://doi.org/10.1002/2016WR019655>, 2017.  
870

871 Severinghaus, J. P., Beaudette, R., Headly, M. A., Taylor, K. and Brook, E. J.: Oxygen-18 of O<sub>2</sub> records  
872 the impact of abrupt climate change on the terrestrial biosphere, *Science*, 324, 1431-1434,  
873 <https://doi.org/10.1126/science.1169473>, 2009.  
874

875 Shackleton, N. J.: The 100,000-Year Ice-Age Cycle Identified and Found to Lag Temperature,  
876 Carbon Dioxide, and Orbital Eccentricity, *Science*, 289, 1897-1902,  
877 <https://doi.org/10.1126/science.289.5486.1897>, 2000.  
878

879 Sharkey, T.D., Badger, M.R., von Caemmerer, S., and Andrews, T.J.: High Temperature Inhibition of  
880 Photosynthesis Requires Rubisco Activase for Reversibility, *Trends Plant Sci.*, 2465-2468,  
881 [https://doi.org/10.1007/978-94-011-3953-3\\_577](https://doi.org/10.1007/978-94-011-3953-3_577), 1998.

882



883 Sharp, Z. D., and Wostbrock, J. A. G.: Standardization for the Triple Oxygen Isotope System: Waters,  
884 Silicates, Carbonates, Air, and Sulfates, *Rev. Mineral. Geochem.*, 86, 179-196,  
885 <https://doi.org/10.2138/rmg.2021.86.05>, 2021.  
886

887 Stolper, D. A., Fischer, W. W., and Bender, M. L.: Effects of temperature and carbon source on the  
888 isotopic fractionations associated with O<sub>2</sub> respiration for <sup>17</sup>O/<sup>16</sup>O and <sup>18</sup>O/<sup>16</sup>O ratios in *E.*  
889 *coli*, *Geochim. Cosmochim. Ac.*, 240, 152-172, <https://doi.org/10.1016/j.gca.2018.07.039>, 2018.

890 Tcherkez, G., and Farquhar, G.D.: On the <sup>16</sup>O/<sup>18</sup>O isotope effect associated with photosynthetic O<sub>2</sub>  
891 production, *Funct. Plant Biol.*, 34, 1049-1052, <https://doi.org/10.1071/FP07168>, 2007.

892 Tcherkez, G., Gauthier, P., Buckley, T.N, Bush, F.A., Barbour, M.M., Bruhn, D., Heskell, M.A., Gong, X.Y.,  
893 Crous, K.Y., Griifin, K., Way, D., Turnbull, M., Adams, M.A., Atkin, O.K., Farquhar, G.D., and Cornic, G.:  
894 Leaf day respiration: low CO<sub>2</sub> flux but high significance for metabolism and carbon balance, *New*  
895 *Phytol.*, 216, 986-1001, <https://doi.org/10.1111/nph.14816>, 2017.

896 Vinogradov, A. P., Kutyurin, V.M., and Zadorozhnyi, I.K.: Isotope fractionation of atmospheric oxygen,  
897 *Geochem. Int.*, 3, 241-253, 1959.

898 Wang, Y., Cheng, H., Lawrence Edwards, R., Kong, X., Shao, X., Chen, S., Wu, J., Jiang, X., Wang, X.,  
899 and An, Z.: Millennial- and orbital-scale changes in the East Asian monsoon over the past 224,000  
900 years, *Nature*, 451, 1090-1093, <https://doi.org/10.1038/nature06692>, 2008.  
901

902 Wostbrock, A. G. J., and Sharp, Z., D.: Triple Oxygen Isotopes in Silica–Water and Carbonate–Water  
903 Systems, *Rev. Mineral. Geochem.*, 86, 367-400, <https://doi.org/10.2138/rmg.2021.86.11>, 2021.  
904